

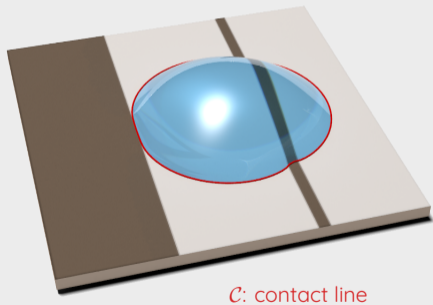
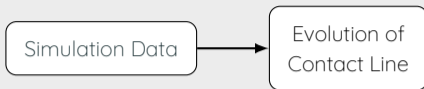
## Task 3.5: AI for wetting hydrodynamics

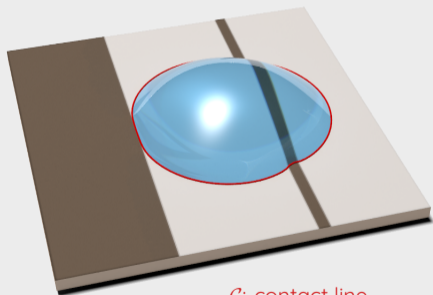
Andreas Demou, Nikos Savva

The Cyprus Institute

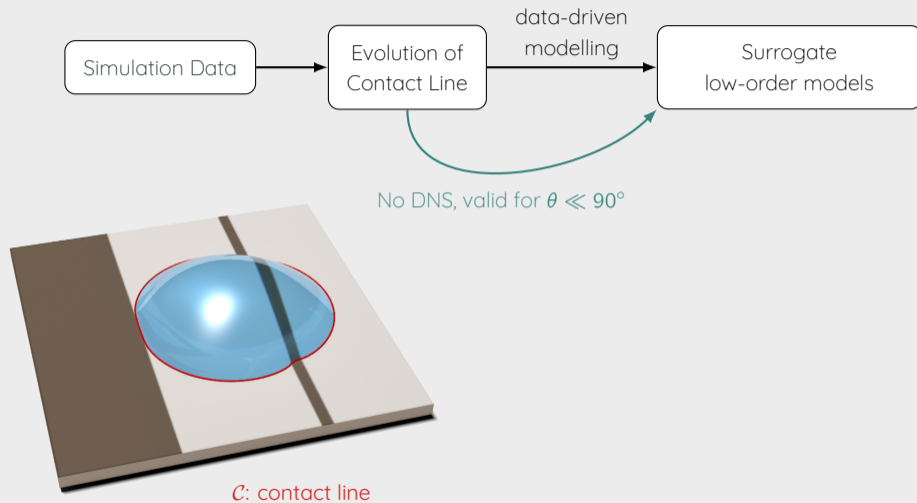
Raise AHM

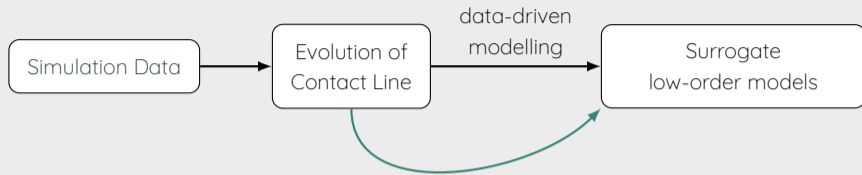
Iceland, August 28, 2023



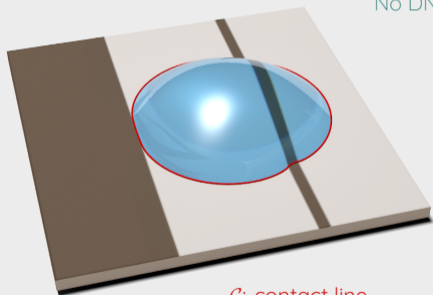


$\mathcal{C}$ : contact line

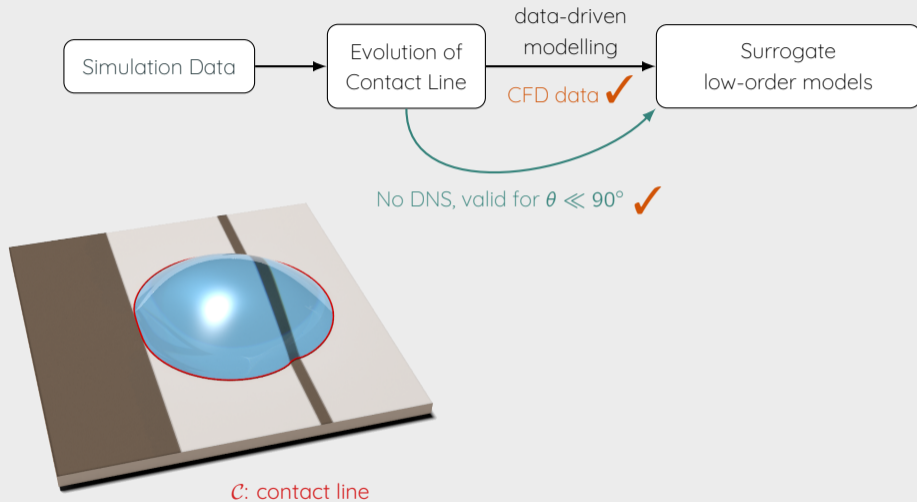


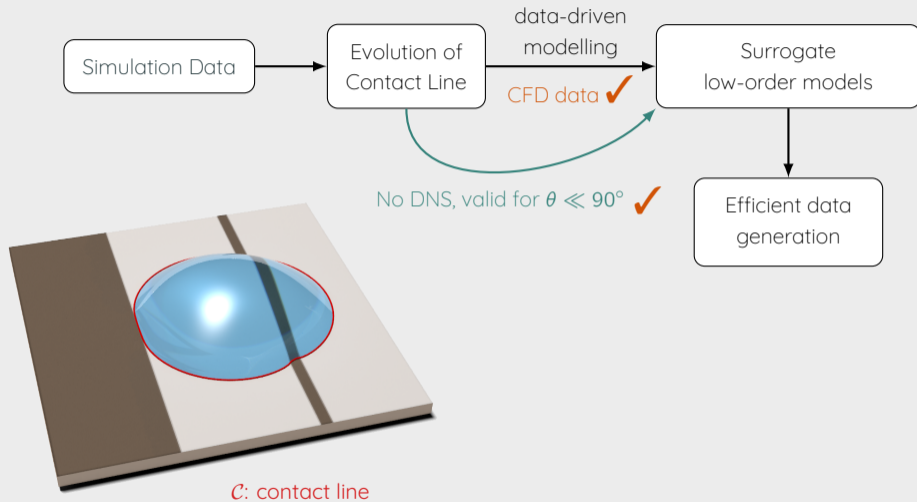


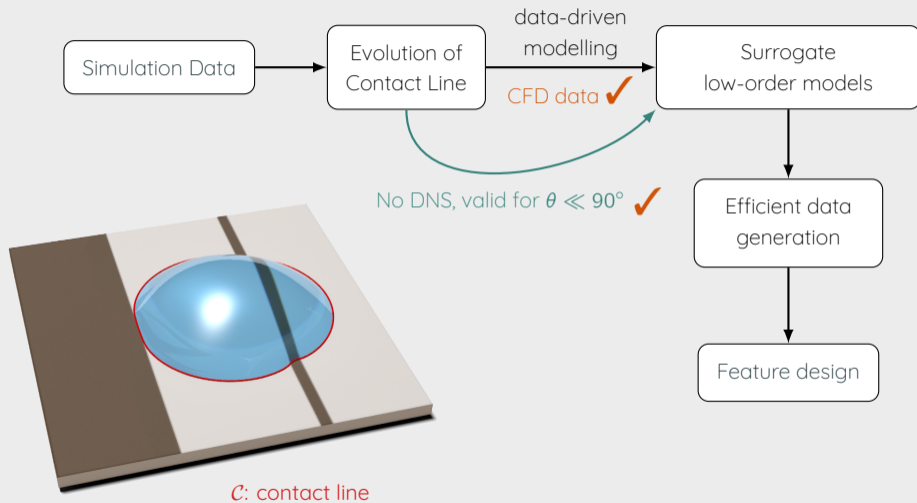
No DNS, valid for  $\theta \ll 90^\circ$  ✓



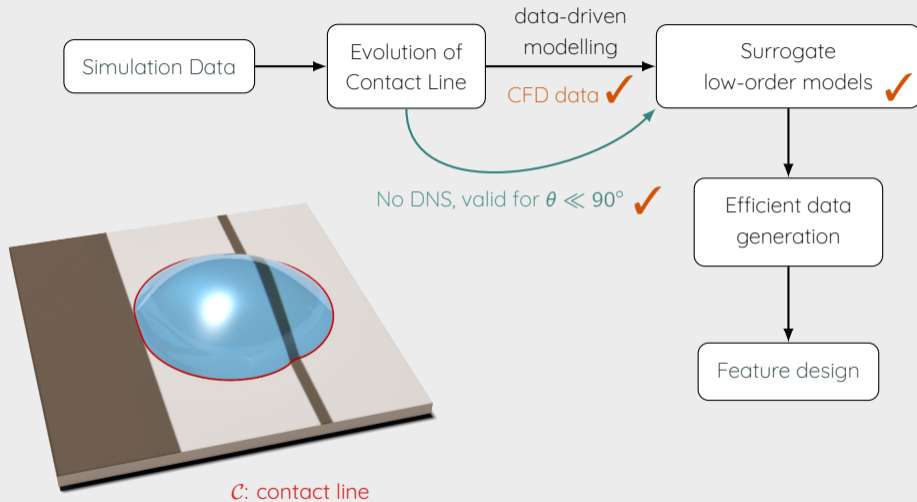
$\mathcal{C}$ : contact line

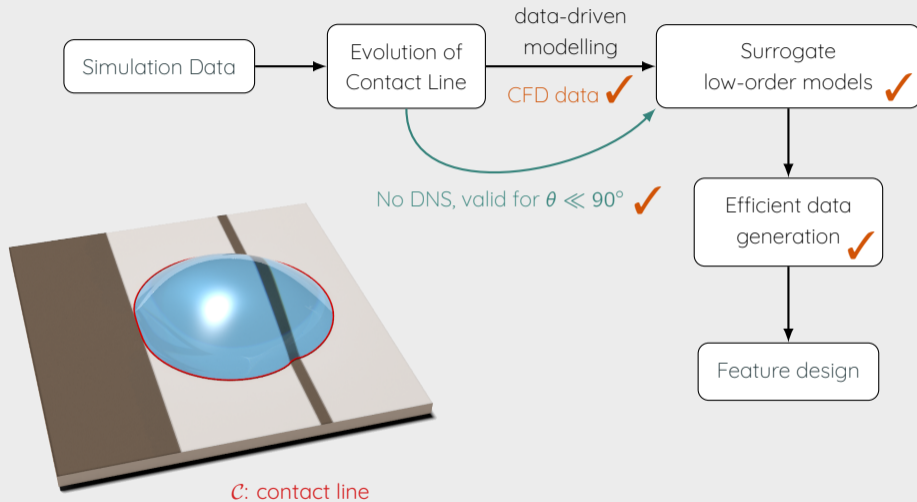


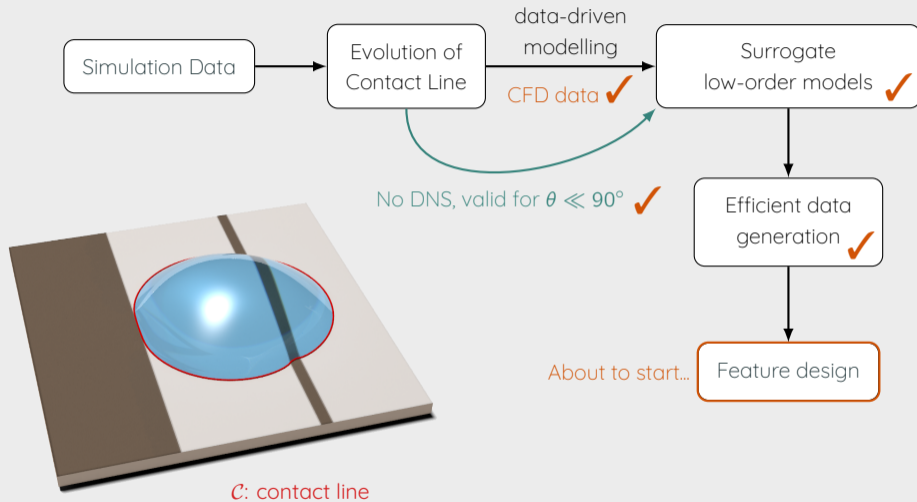












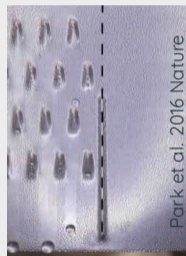
- Industry

- Pesticide deposition
  - Coating processes
  - Wetting agents



- Technology

- Inkjet printing
  - Microfluidic & lab-on-a-chip devices
  - Display technologies



- Surface design

- Surface cleaning
  - Waterproofing
  - Water harvesting



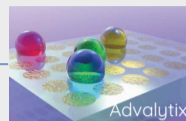
- Energy

- Oil recovery
  - Fuel cells
  - Mechanical Energy harvesting



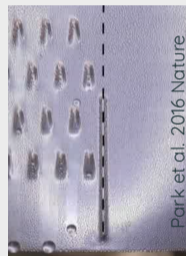
- Industry

- Pesticide deposition
  - Coating processes
  - Wetting agents



- Technology

- Inkjet printing
  - Microfluidic & lab-on-a-chip devices
  - Display technologies



- Surface design

- Surface cleaning
  - Waterproofing
  - Water harvesting

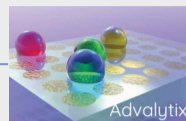
- Energy

- Oil recovery
  - Fuel cells
  - Mechanical Energy harvesting



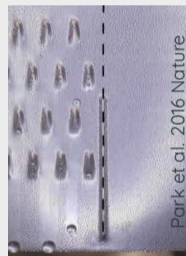
- Industry

  - Pesticide deposition
  - Coating processes
  - Wetting agents



- Technology

  - Inkjet printing
  - Microfluidic & lab-on-a-chip devices
  - Display technologies



- Surface design

  - Surface cleaning
  - Waterproofing
  - Water harvesting



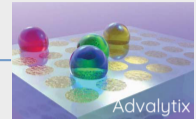
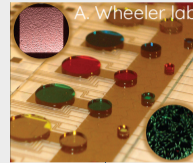
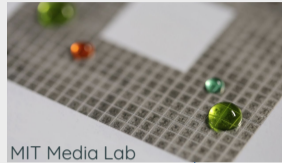
- Energy

  - Oil recovery
  - Fuel cells
  - Mechanical Energy harvesting



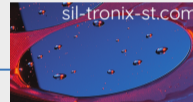
- Industry

  - Pesticide deposition
  - Coating processes
  - Wetting agents



- Technology

  - Inkjet printing
  - Microfluidic & lab-on-a-chip devices
  - Display technologies



- Surface design

  - Surface cleaning
  - Waterproofing
  - Water harvesting



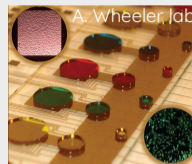
- Energy

  - Oil recovery
  - Fuel cells
  - Mechanical Energy harvesting



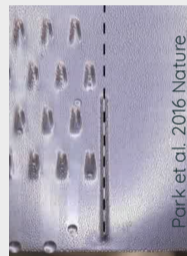
- Industry

  - Pesticide deposition
  - Coating processes
  - Wetting agents



- Technology

  - Inkjet printing
  - Microfluidic & lab-on-a-chip devices
  - Display technologies



- Surface design

  - Surface cleaning
  - Waterproofing
  - Water harvesting



- Energy

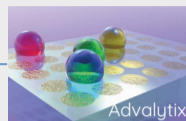
  - Oil recovery
  - Fuel cells
  - Mechanical Energy harvesting





- Industry

- Pesticide deposition
  - Coating processes
  - Wetting agents

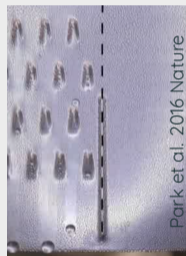


- Technology

- Inkjet printing
  - Microfluidic & lab-on-a-chip devices
  - Display technologies

- Surface design

- Surface cleaning
  - Waterproofing
  - Water harvesting



- Energy

- Oil recovery
  - Fuel cells
  - Mechanical Energy harvesting



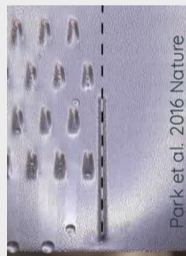
- Industry

- Pesticide deposition
  - Coating processes
  - Wetting agents



- Technology

- Inkjet printing
  - Microfluidic & lab-on-a-chip devices
  - Display technologies



- Surface design

- Surface cleaning
  - Waterproofing
  - Water harvesting

- Energy

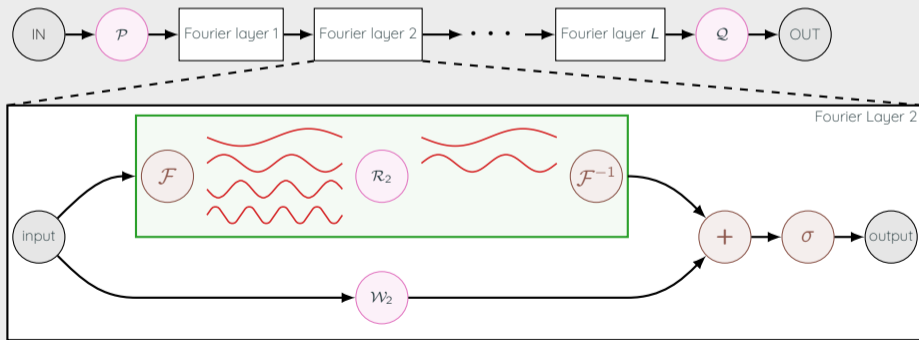
- Oil recovery
  - Fuel cells
  - Mechanical Energy harvesting



Learn contact line dynamics in a data-driven manner, by considering the mapping:

$$G = (\text{aux. data}) \rightarrow \{\text{Solution}\}$$

**Key idea:** A neural operator can approximate  $G$  through the Fourier space.



**Completed work**  
**Modelling thin-film data**

---

## Assumptions

- strong surface tension
- negligible inertial effects
- small contact angles

## Non-dimensional governing PDE

$$\partial_t h + \nabla \cdot [h(h^2 + \lambda^2)\nabla \nabla^2 h] = 0$$

## Boundary conditions along the contact line $\mathcal{C}$ ( $\nu$ is the unit outward normal on $\mathcal{C}$ )

Thickness vanishes:  $h|_{\mathcal{C}} = 0$

Contact angle:  $|\nabla h|_{\mathcal{C}} = -h_\nu = \vartheta_*$

Kinematic BC:  $(\partial_t \mathbf{c} - \lambda^2 \nabla \nabla^2 h|_{\mathcal{C}}) \cdot \nu = 0$

Contact line  $\mathbf{c}(t_i)$  is discretised with 128 points and time  $t_i$  is discretised uniformly.

## Auto-regressive approach

Input:  $\{\mathbf{c}(t_1), \mathbf{c}(t_2), \dots, \mathbf{c}(t_{10}), \vartheta_*(t_1), \vartheta_*(t_2), \dots, \vartheta_*(t_{10})\}$

Output:  $\mathbf{c}(t_{11})$ , i.e. subsequent solution

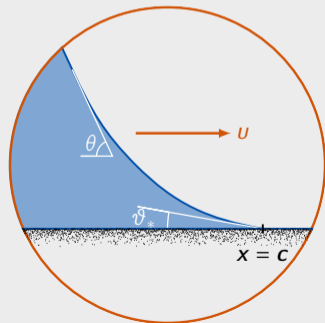
## AI-assisted, hybrid approach

Droplet velocity normal to the contact line,  $u_\nu$ ,

$$u_\nu = \bar{u}_\nu + G(\mathbf{c}, \bar{u}_\nu) \quad \text{with} \quad \bar{u}_\nu = \frac{\theta^3 - \vartheta_*^3}{3 |\ln \lambda|}$$

Input:  $\{\mathbf{c}(t_i), \bar{u}_\nu(t_i)\}$

Output:  $G(\mathbf{c}, \bar{u}_\nu)$



Contact line  $\mathbf{c}(t_i)$  is discretised with 128 points and time  $t_i$  is discretised uniformly.

## Auto-regressive approach

Input:  $\{\mathbf{c}(t_1), \mathbf{c}(t_2), \dots, \mathbf{c}(t_{10}), \vartheta_*(t_1), \vartheta_*(t_2), \dots, \vartheta_*(t_{10})\}$

Output:  $\mathbf{c}(t_{11})$ , i.e. subsequent solution

## AI-assisted, hybrid approach

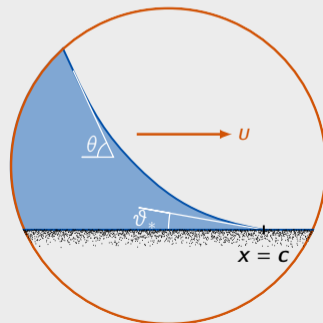
Droplet velocity normal to the contact line,  $u_\nu$ ,

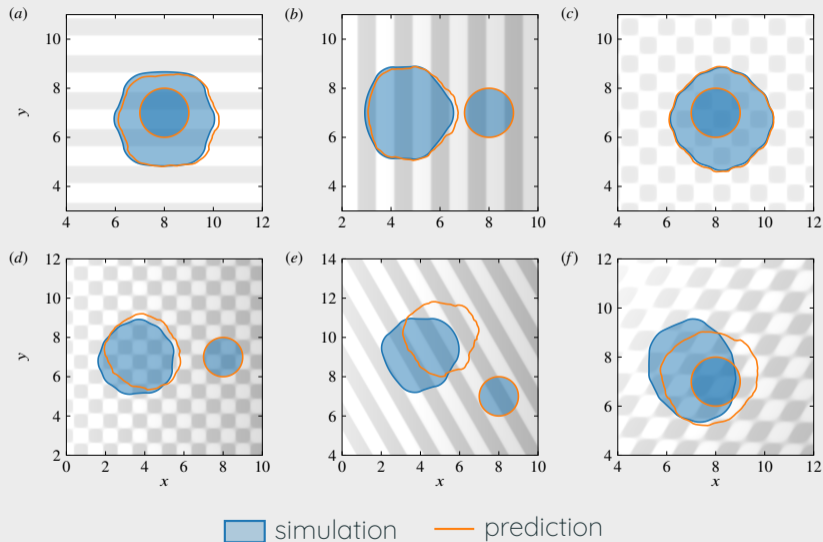
$$u_\nu = \bar{u}_\nu + G(\mathbf{c}, \bar{u}_\nu) \quad \text{with} \quad \bar{u}_\nu = \frac{\theta^3 - \vartheta_*^3}{3 |\ln \lambda|}$$

Input:  $\{\mathbf{c}(t_i), \bar{u}_\nu(t_i)\}$

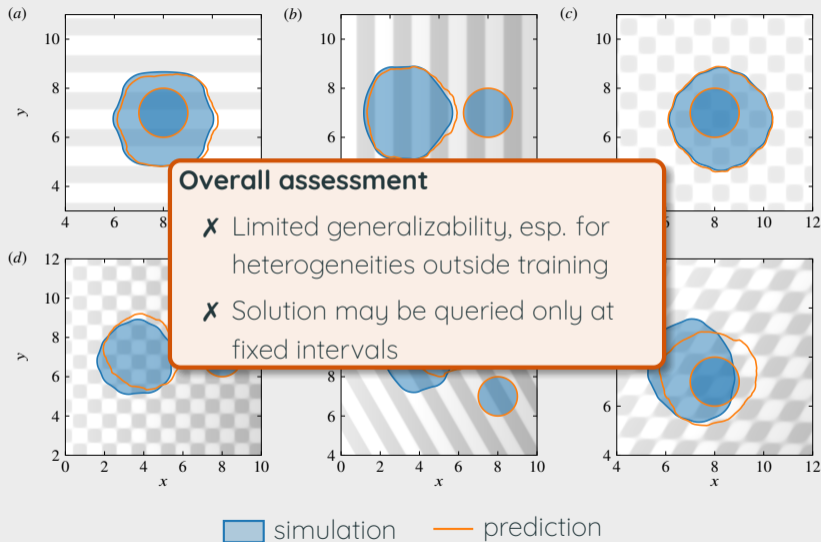
Output:  $G(\mathbf{c}, \bar{u}_\nu)$

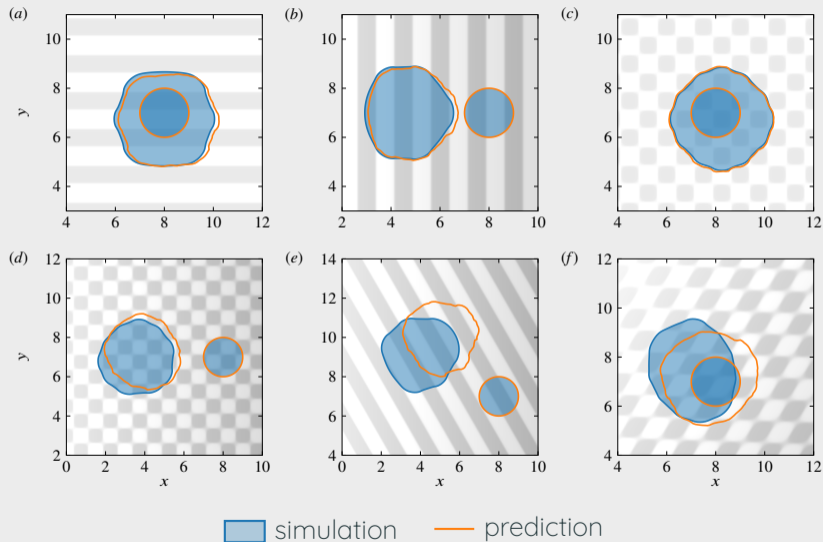
data-driven, implicit in  $t$

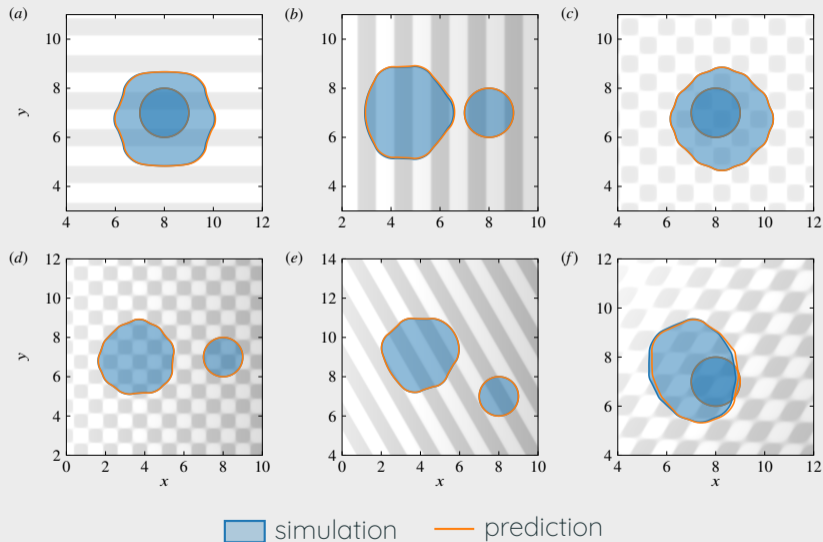


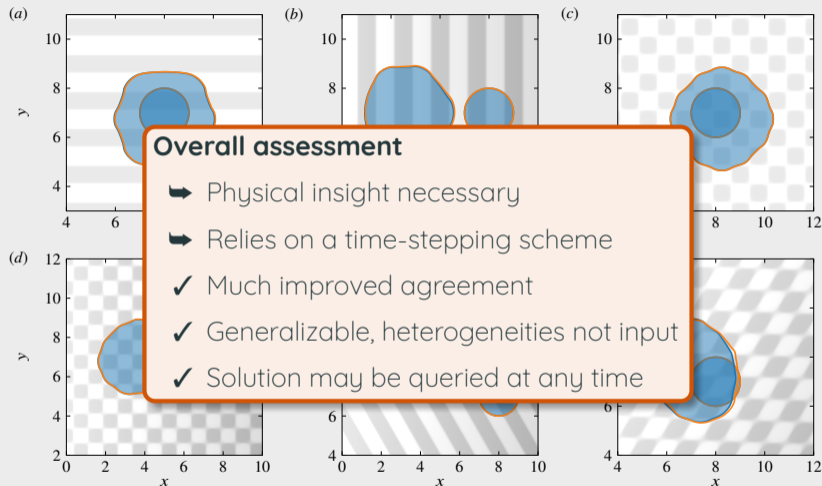








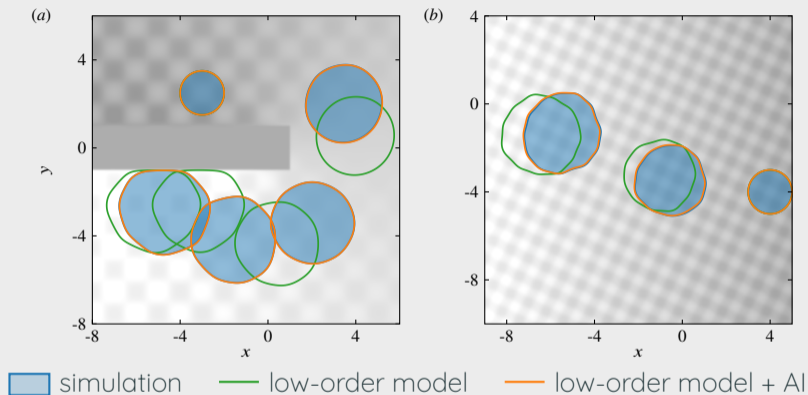




### Overall assessment

- ➔ Physical insight necessary
- ➔ Relies on a time-stepping scheme
- ✓ Much improved agreement
- ✓ Generalizable, heterogeneities not input
- ✓ Solution may be queried at any time

simulation
  prediction



Under review in **Data-centric Engineering** (Cambridge University Press)

Reviewer: "This paper is absolutely excellent. It is well-written and convincing. It should be accepted."

**On-going work**  
**Modelling CFD data**

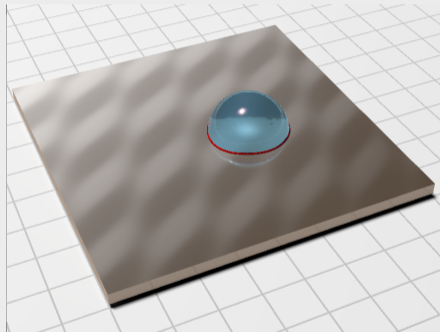
---

## Code: Basilisk

- random heterogeneities, from a 7-parameter functional form
- 10–50 dimensionless times, snapshot saved every 0.1 time units
- adaptive mesh refinement, local grid size between  $1/2^5 - 1/2^8$

## Dataset:

- 300 DNS cases
- 80,000 contact line snapshots



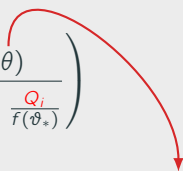
Analysis near the contact line reveals

$$u_\nu^{COX} = \frac{\sigma}{\mu} \left( \frac{F(\vartheta_*) - F(\theta)}{\ln\left(\frac{\lambda}{r_0}\right) + \frac{Q_o}{f(\theta)} - \frac{Q_i}{f(\vartheta_*)}} \right)$$

- $\lambda$ , slip length, scales with  $\Delta x$
- $\sigma$  surface tension;  $\mu$  viscosity
- $Q_o$  and  $Q_i$  are **unspecified**
- $F$  and  $f$  are **known**



Analysis near the contact line reveals

$$u_\nu^{COX} = \frac{\sigma}{\mu} \left( \frac{F(\vartheta_*) - F(\theta)}{\ln\left(\frac{\lambda}{r_0}\right) + \frac{Q_o}{f(\theta)} - \frac{Q_i}{f(\vartheta_*)}} \right)$$


- $\lambda$ , slip length, scales with  $\Delta x$
- $\sigma$  surface tension;  $\mu$  viscosity
- $Q_o$  and  $Q_i$  are **unspecified**
- $F$  and  $f$  are **known**

## Obtaining $\theta$ assuming quasi-static dynamics

Given  $\mathbf{c}$ , obtain  $\theta$  from the slope of the solution to the Young–Laplace eqn

$$-\sigma \nabla \cdot \hat{\mathbf{n}} = \Delta p, \quad \hat{\mathbf{n}} \text{ the surface unit normal}$$

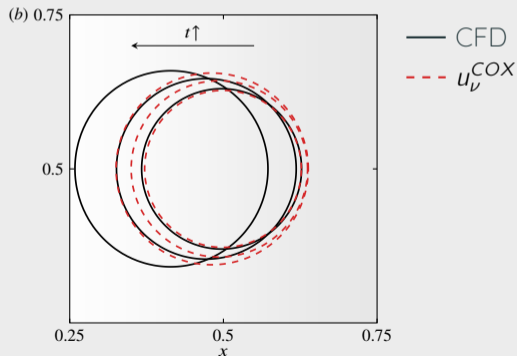
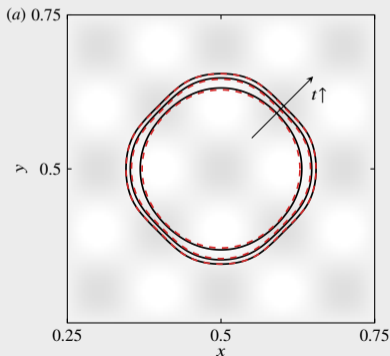
$\Delta p$  is constant specified by the volume constraint.

➔ Using the open source code, **Surface Evolver** (SE). Repeated calls to SE during training/testing through a dedicated Python interface.

Analysis near the contact line reveals

$$u_{\nu}^{COX} = \frac{\sigma}{\mu} \left( \frac{F(\vartheta_*) - F(\theta)}{\ln\left(\frac{\lambda}{r_0}\right) + \frac{Q_o}{f(\theta)} - \frac{Q_i}{f(\vartheta_*)}} \right)$$

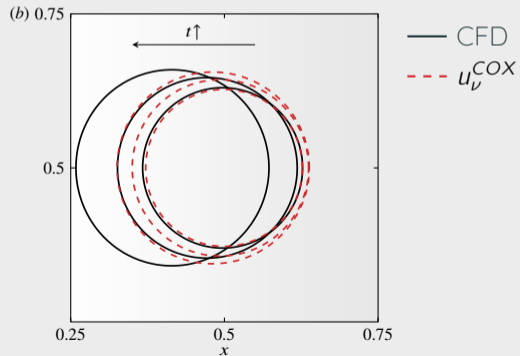
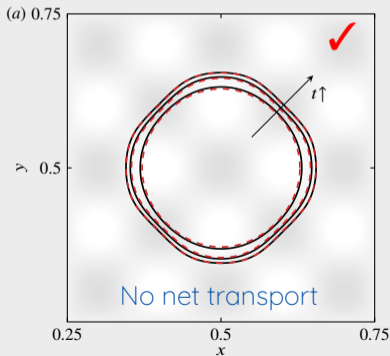
- $\lambda$ , slip length, scales with  $\Delta x$
- $\sigma$  surface tension;  $\mu$  viscosity
- $Q_o$  and  $Q_i$  are **unspecified**
- $F$  and  $f$  are **known**



Analysis near the contact line reveals

$$u_v^{COX} = \frac{\sigma}{\mu} \left( \frac{F(\vartheta_*) - F(\theta)}{\ln\left(\frac{\lambda}{r_0}\right) + \frac{Q_o}{f(\theta)} - \frac{Q_i}{f(\vartheta_*)}} \right)$$

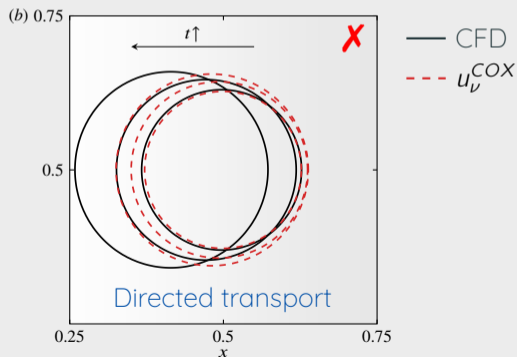
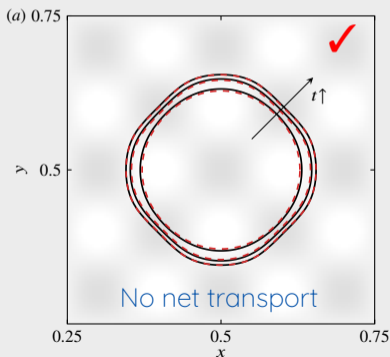
- $\lambda$ , slip length, scales with  $\Delta x$
- $\sigma$  surface tension;  $\mu$  viscosity
- $Q_o$  and  $Q_i$  are **unspecified**
- $F$  and  $f$  are **known**



Analysis near the contact line reveals

$$u_v^{COX} = \frac{\sigma}{\mu} \left( \frac{F(\vartheta_*) - F(\theta)}{\ln\left(\frac{\lambda}{r_0}\right) + \frac{Q_o}{f(\theta)} - \frac{Q_i}{f(\vartheta_*)}} \right)$$

- $\lambda$ , slip length, scales with  $\Delta x$
- $\sigma$  surface tension;  $\mu$  viscosity
- $Q_o$  and  $Q_i$  are **unspecified**
- $F$  and  $f$  are **known**



Analysis near the contact line reveals

- $\lambda$ , slip length, scales with  $\Delta x$

$$u_v^{COX} = \frac{\sigma}{\mu} \left( \frac{F(\vartheta)}{\ln\left(\frac{\lambda}{r_0}\right)} \right)$$

**Cox's model underestimates net transport**

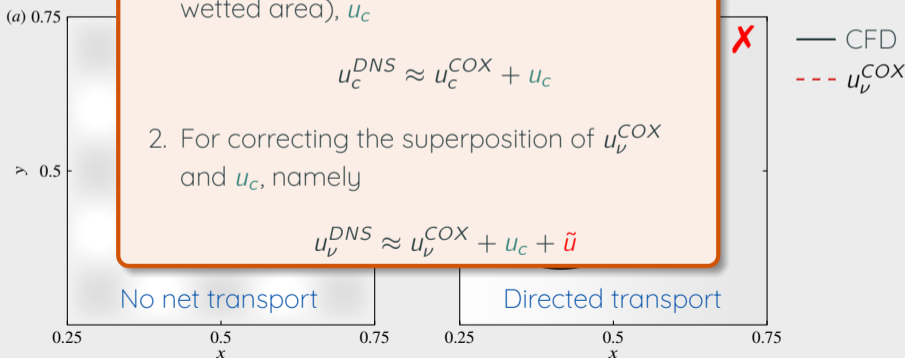
**Approach: train two models**

1. For net transport (speed of the centroid of wetted area),  $u_c$

$$u_c^{DNS} \approx u_c^{COX} + u_c$$

2. For correcting the superposition of  $u_v^{COX}$  and  $u_c$ , namely

$$u_v^{DNS} \approx u_v^{COX} + u_c + \tilde{u}$$



Net transport captured by first harmonic; contact line evolves such that contact line has no first harmonic

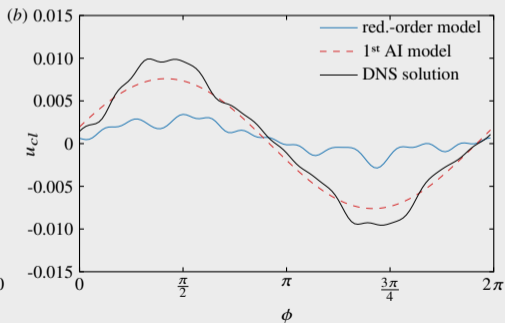
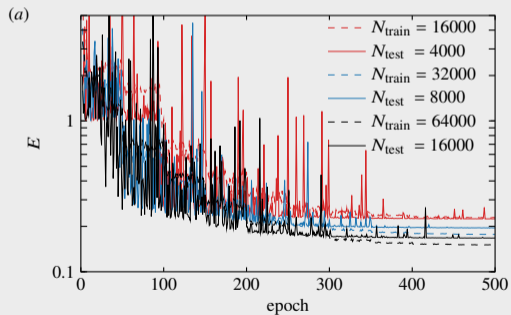
**Input:** snapshots of first harmonics of  $\theta$  and  $\vartheta_*$

**Output:** snapshots of first harmonics of  $u_\nu^{DNS} - u_\nu^{COX} = u_c^{DNS} - u_c^{COX} \rightarrow u_c$

Net transport captured by first harmonic; contact line evolves such that contact line has no first harmonic

**Input:** snapshots of first harmonics of  $\theta$  and  $\vartheta_*$

**Output:** snapshots of first harmonics of  $u_v^{DNS} - u_v^{COX} = u_c^{DNS} - u_c^{COX} \rightarrow u_c$



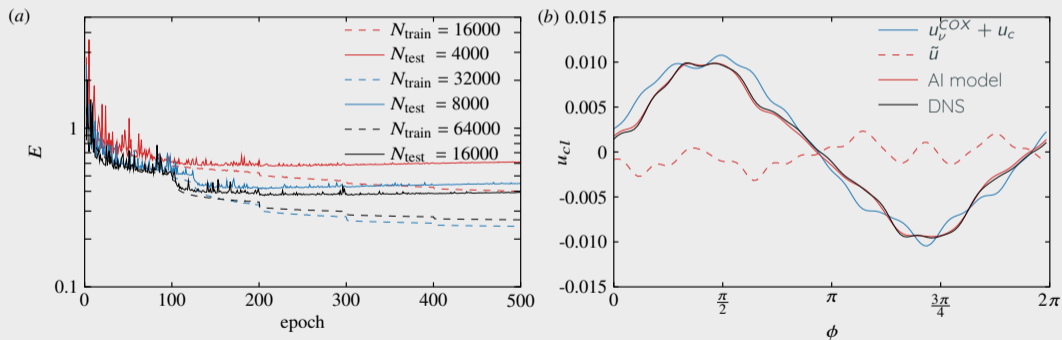
**Input:** snapshots of  $\{\mathbf{c}, u_\nu^{COX} + u_c\}$

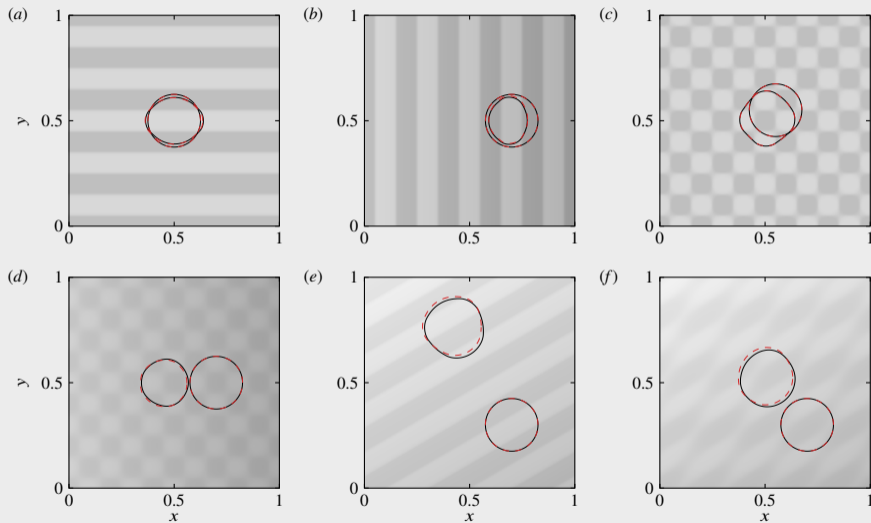
**Output:** snapshots of  $u_\nu^{DNS} - (u_\nu^{COX} + u_c) \rightarrow \tilde{u}$

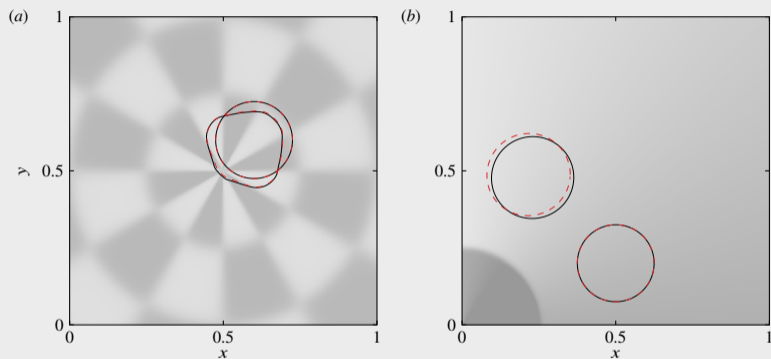


**Input:** snapshots of  $\{\mathbf{c}, u_\nu^{\text{COX}} + u_c\}$

**Output:** snapshots of  $u_\nu^{\text{DNS}} - (u_\nu^{\text{COX}} + u_c) \rightarrow \tilde{u}$







Paper in preparation, to be submitted in the coming weeks.

## Future tasks

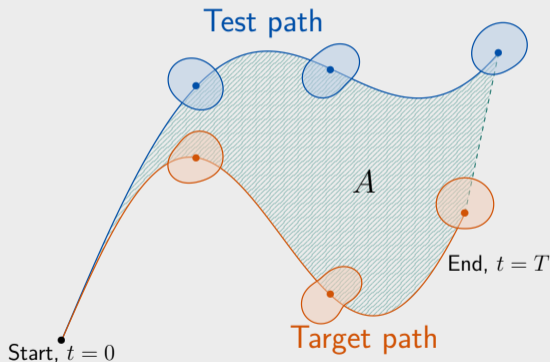
---

## Employ similar workflow:

$$u_\nu = u_\nu^{COX} + u_c + \tilde{u}$$

- $u_\nu^{COX}$  - function of  $(\theta, \vartheta_*, r)$ .
  - $u_c$  - for net transport as a function of the first harmonics of  $(\theta, \vartheta_*)$  and the gravity vector.
  - $\tilde{u}$  - for higher-order corrections as a function of  $(\mathbf{c}, u_\nu^{COX} + u_c)$ .
- 
- Currently post-processing data from 100 extra DNS for inclined surfaces.
  - Further analytical understanding may be necessary.

Given a target droplet path, what heterogeneity profile  $\vartheta_*$  can induce it?



General het. profile given by:

$$\vartheta_* = \sum_{m,n} a_{m,n} \exp^{ik_m x + ik_n y},$$

$a_{m,n}$  'design' variables

Optimisation procedure to obtain:

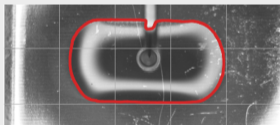
$$a_{m,n}^* = \operatorname{argmin} J$$

where  $J$  is a cost function that depends on  $A$  and some metric that penalizes non-circular contact lines

## Successes enabled by RAISE

---

- **Research funding:** three successful proposals involving AI for wetting projects  
2 EU-funded MSCA ITNs; 1 CY-Funded Excellence Hubs project as PI
- **Computing time grants:** three successful proposals for computing time.  
1 under EuroHPC JU\*; 2 on the national machine  
\*to be featured in EuroHPC JU's "success stories" webpage
- **Industrial collaboration** with a tribology R&D company in Austria



Surface texturing effectively guides lubricant flow  
CFD simulations infeasible (micron-scale texturing to centi-metre scale drops)  
Develop reduced-order surrogates to inform texture design



drive. enable. innovate.



The CoERAISE project have received funding from the European Union's Horizon 2020 – Research and Innovation Framework Programme H2020-INFRAEDI-2019-1 under grant agreement no. 951733

**Extra slides**

---

## Two-phase Stokes

$$\begin{aligned}\vec{\nabla} \cdot \vec{u} &= 0, \\ \rho \frac{\partial \vec{u}}{\partial t} &= -\vec{\nabla} p + \vec{\nabla} \cdot [\mu (\vec{\nabla} \vec{u} + \vec{\nabla} \vec{u}^T)] + \sigma \kappa \delta_{\Gamma} \vec{n} + \hat{\rho} \vec{g}, \\ \frac{\partial C}{\partial t} + \vec{\nabla} \cdot (\vec{u} C) &= 0, \text{ where } C(\vec{x}, t) = \begin{cases} 1 & \text{if } \vec{x} \in \text{liquid,} \\ 0 & \text{if } \vec{x} \in \text{gas.} \end{cases}\end{aligned}$$

**Physical properties  $\xi$  calculation:**  $\xi(\vec{x}, t) = \xi_1 C(\vec{x}, t) + \xi_2 (1 - C(\vec{x}, t))$ .

**Boundary conditions:** impose local contact angle (chemical heterogeneity) on surface.